Tech Science Press

The Effect of the Process on Mechanical Properties of Polylactic Acid-Date Palm Leaf Fibers Composite Films Produced By Extrusion Blowing

Fatma Kharrat[1], Rania Chaari[1], Mohamed Khlif[1], Loic Hilliou[2], José A. Covas[2], Mohamed Haboussi[3,*], Hedi Nouri[1] and Chedly Bradai[1]

[1]National School of Engineers of Sfax (ENIS), Laboratory of Electromechanical Systems (LASEM), B.P.W. 3038, Sfax, Tunisia.

[2]Institute for Polymers and Composites, University of Minho, Guimarães, Portugal.

[3]Laboratoire des Sciences des Procédés et des Matériaux (LSPM), CNRS UPR 3407, Université Paris 13, Sorbonne-Paris-Cité, 93430, Villetaneuse, France.

[*]Corresponding Author: Mohamed Haboussi. Email: haboussi@univ-paris13.fr.

Abstract: Biocomposite films prepared with melt compounding and film blowing have become a new trend in plastic research to deliver more eco-friendly packages. Polylactic acid (PLA) was melt compounded with minimally processed date palm leaf fiber (DPLF) and converted into films by blown film extrusion. The compounding was done in order to enhance the film mechanical properties in one hand, and to decrease the film production cost in the other hand. In this present study, a reference PLA film and films with 1%, 2%, and 5% of DPLF (weight %) were produced with different process parameters. The spatial variations in films thickness and lay flat width indicate that the addition of DPLF up to 2% enhances the bubble stability for the tested process parameters. However, the composite with 5% DPLF shows nearly the same processability window as the neat PLA. The structural and mechanical characterizations of films suggest a reinforcing effect of the PLA matrix up to 2% of fiber (with an optimum at 1%). Larger DPLF loading leads to depressed and more anisotropic mechanical properties, related to an increased density of defects at the fiber-PLA fragile interface and to a DPLF-induced enhanced PLA thermal degradation and amorphous phase orientation.

Keywords: PLA; palm leaf fibers; biocomposites; film blowing

1 Introduction

In the last years, a considerable research effort has been dedicated to the formulation and characterization of new ecologically friendly plastic materials for packaging application. Among the various biopolymers known, polylactic acid (PLA) has owned a particular interest by the industries due to its biodegradability, biocompatibility and renewability [1-7]. PLA has relatively high modulus and strength. However, drawbacks like high cost, inherent brittleness, low melt strength and poor thermal stability are still limiting its industrial use and application in converting technologies. Consequently, recent research and development in modification of PLA comprising melt blending with biodegradable polymers or compounding with chain modifiers or additives has bloomed in order to improve PLA properties [8-10]. Several efforts have been devoted to incorporate various fillers in PLA matrix in order to improve the products' properties while reducing their cost. It has been reported that natural fibers composites exhibit mechanical performances, including high strength and stiffness, which compare well to synthetic fibers composites [5]. Moreover, the use of natural fibers is very promising for the production of materials with low environmental impact, better eco-friendliness and lower cost.

Despite the vast literature on PLA based biocomposites with natural fillers [11-19], only few studies have been devoted to the development of materials for extrusion film blowing, a converting process which is widely spread in the film packaging industry. In this peculiar line of research, polysaccharide

nanocrystals have been largely used as filler for PLA nanocomposite film production [20-22]. To the best of our knowledge, the use of a minimally processed natural waste fiber for reinforcing PLA in film blowing application is not yet documented in the literature.

The date palm (Phoenix dactylifera) is one of the most cultivated palms in the arid and semi-arid regions of the world. Tunisia has approximately 5,5 million trees of date palm, covering an area of 40 976 ha [23]. The removal of dry leaves after harvesting generates an important quantity of date palm leaves residues amounting to more than 198 000 tons accumulated every year in Tunisian agricultural lands [24]. A rational way of valorizing this abundant renewable resource could be its use as reinforcing fibers in polymeric composite materials. Thus, the aim of the present work was the extrusion film blowing of a PLA matrix reinforced with natural fiber (date palm leaf fiber, DPLF) with the purpose to enhance the film mechanical properties in one hand, and to decrease the film production cost in the other hand. PLA biocomposites incorporating different amounts of DPLF were first melt compounded. Then the processability of the biocomposites into blown films was investigated by screening the effects of selected processing parameters on the bubble stability. Stable bubbles were obtained and the resulting films were characterized to assess the impact of DPLF content on the film properties.

2 Materials and Methods

2.1 Materials

Date palm leaves used in this study were gathered from the waste of date harvesting in the region of Kébeli, located in southern Tunisia, in the period of October-December 2016. These remains were received grinded. A first sieve was done in order to remove big size wastes to make the grinding process easier. Then, fibers were grinded in a hammer mill and finally sieved using a laboratory test sieve (MATEST) with a mesh of 80 µm.

PLSF 101 was bought from Nature plast. It is a PLA based thermoplastic designed for extrusion film blowing, and made from renewable vegetal sources.

2.2 Methods

2.2.1 Preparation of PLA/DPLF Composites and Film Blowing

PLA/DPLF composites were produced with a Leistritz LSM 34 GL co-rotating twin-screw extruder (L/D = 29; D = 34 mm). Pellets of PLA were first dried for three hours in air convection oven at 70°C. Then, premixes of PLA and DPLF at the target composition were fed at a rate of 4 kgs/h in the hopper of the extruder with a volumetric feeder (Moretto DVM18-L). Residual moisture and volatiles were removed though a venting port located at L/D = 23. A water bath was used to cool the extrudate, which was then dried with an air-knife and finally pelletized by a rotary cutter.

Composites pellets with different fiber concentration were fed in an extrusion film blowing lab scale machine (Periplast, Portugal) described at length elsewhere [25]. Several process conditions were varied for each compound in view of testing their impact on the bubble stability, whereas the cooling conditions were similar for all the bubbles. The varied processing parameters are the extruder temperature profile (three zones for the die and three zones for the extruder), the screw speed, the nip roll velocity (V_n) (see Fig. 1) and the bubble insufflation. All process conditions of produced films are given in Tab. 1. Different temperature profiles were adopted to cope with variations in the rheological properties of the PLA/DPLF composites. The blow up ratio, BUR, quantifies the biaxial stretching of the material due to the air pressure in the bubble. BUR is given by the following expression:

$$BUR = \frac{Df}{Dd} \tag{1}$$

where D_f is the bubble diameter and D_d is the diameter of the die lips. The take up ratio, TUR, is adjusted by both the extrusion velocity and the nip rolls velocity and quantifies the stretching of the material along the machine direction (MD). TUR is given by the following expression:

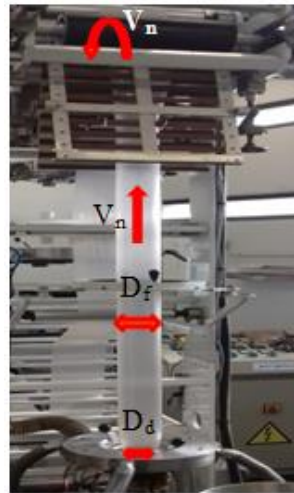$$TUR = \frac{Width\ of\ Die\ Gap}{Film\ Thickness \times BUR} \tag{2}$$

Figure 1: Film blowing of neat PLA. V_n indicates the velocity of the nip rolls which take up the bubble. D_f (which relates to the amount of air insufflated in the bubble) and D_d are defined in Eq. (1)

Table 1: Processing conditions of blown films (BUR, blow-up ratio; TUR, take-up ratio; DDR, drawdown ratio defined as the product of BUR and TUR) and respective films crystallinity X (in %) measured from wide angle X-ray scattering performed along MD and TD

Fiber content (wt.%)	Set temperature profile from die to hopper (°C)	Screw speed (rpm)	Nip rolls velocity (m/min)	BUR	TUR	DDR	X in MD	X in TD
0	165/175/175/190/185/185	35	2.8	1.8	10.7	19.3		
	150/165/175/185/185/185	35	5.5	2.0	19.8	39.6		
		45	4	2.3	11.2	25.8	50.4 ± 1.6	49.3 ± 1.8
1	165/180/180/185/185/185	70	4	1.9	7.1	13.5		
		45	4	1.9	9.0	17.1	41.8 ± 2.5	41.6 ± 1.3
2	165/175/175/190/190/185	45	4	1.8	7.7	13.9	37.4 ± 0.2	35.9 ± 0.9
	160/175/175/190/185/185	35	4	1.6	9.3	14.9		
		70	4	1.5	7.1	10.6		
5		45	4	1.4	8.9	12.5		
	150/165/165/175/180/180	45	4,5	1.8	9.0	16.2		
		45	4,8	2.0	7.2	14.4	27.9 ± 2	27.9 ± 1.8

2.2.2 Films Characterization

The mechanical and morphological properties of selected films in Tab. 1 were characterized. The crystallinity of these films was assessed with wide angle X-ray diffraction (WAXD) using a Bruker D8 Discover diffractometer (λ = 0.154 nm) and scanning from $2\theta = 5°$ to $40°$ with a resolution of 0.04°. Spectra were recorded both in the machine (MD) and transverse directions (TD) of the films and at two different locations along the MD and TD for each film, in order to check for possible structural anisotropy and take into account bubble instabilities and inherent local variations in the film crystalline structure.

Tensile tests of the films were carried out using MTS machine. Rectangular film strips with gauge length of 90 mm and width of 26 mm were cut in the machine direction (MD) and transverse (TD) direction. The tensile speed was set at 10 mm/min and the film thickness was taken as the mean of five measurements along the length of the specimens using a one-micron-resolution micrometer.

Fractured sections of film samples used during tensile testing were imaged with JSM scanning electron microscope (JSM-5400) with an acceleration voltage of 15 kV in order to examine the internal structure of the film.

To investigate the dispersion and the distribution of the fibers in the PLA matrix, optical microscopy of film samples was carried out using a Zeiss Scope A1 AXIO microscope.

3 Results and Discussions

3.1 Film Blowing

Fig. 2 shows photos of composite films with 1% and 5% (in weight) of fiber. The latter exhibits alternating dark and light bands parallel to the MD and a supplementary MD wrinkle in the backside of the film. These bands and wrinkles, also mentioned in other references [26-28], could reflect either a non-homogeneous fiber distribution along TD and/or a variation in film thickness along this direction due to bubble instability during the film blowing process [26]. The absence of (distinctive and visible) bands in the film with 1% suggests either a better fiber distribution or a more uniform thickness along TD. Alternatively, the smaller amount of fiber does not bring the optical contrast necessary to the visualization of the alteration in transparency.
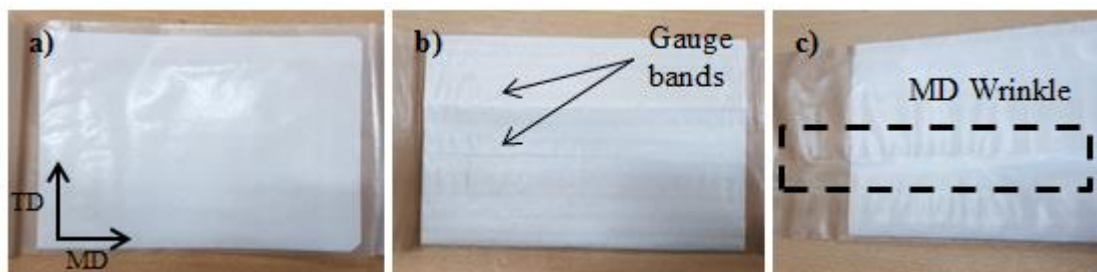

Figure 2: Photos of films with (a) 1% of fiber and (b) 5% of fiber. (c) back side of the 5% film

Bubble stability during blowing is mirrored in the spatial variation of films' thicknesses and lay flat widths. The average films thicknesses along MD and TD and the average lay flat width are presented in Figs. 3(a)-3(c), respectively, for all produced films. The thickness statistics along MD were computed from 6 measurements performed in the middle of the film lay flat width every 20 cm along one meter of length. For the statistics along TD, the film thickness was measured every 2 cm along the lay flat width and the measurements were repeated every 20 cm along one meter in MD. The means and errors of the lay flat widths were determined from the widths measured every 10 cm along 1meter length of the film.

The addition of 1% of DPLF has a stabilizing effect in film blowing process. This is evident when comparing reference PLA film and 1% composite film produced under nearly identical conditions (0%_1.8_10.1 and 1%_1.9_9 films) as the thickness error bars decrease with a simple addition of 1% of fiber. Further addition of fibers go with the enhanced stability of films as error bars computed from films produced under nearly the same conditions (1%_1.9_7.1, 2%_1.8_7.7 and 5%_2_7.2 films) decrease when increasing the fiber rate. The results gathered in Fig. 3 further suggest that an increase in BUR stabilizes the bubbles (see films with 5% DPLF and blown with a TUR of 8.9 or 9). Similar to this, reference PLA films produced with a BUR of 1.8 and 2 and the two 1% DPLF films produced with BUR of 1.9 show that an increase in TUR enhances the bubble stability (compare errors in thicknesses and in the lay flat width). A similar conclusion was drawn from a study carried out with a series of commercial PLA [29]. Nevertheless, the error bars in Fig. 3(b) are significantly larger than in Fig. 3(a), which suggests that bubble instabilities are larger along TD. This observation is supported by the comparison between the spatial variation of film thickness along MD and along TD, reported in Fig. 4. Fig. 4(b), shows a large thickness variation along TD. Zones with reduced thickness will act as a weak point and a zone of a stress concentration when the sample is under loading that can accelerate its break-up. This fact can lead to apparent lower mechanical properties in TD than in MD. In Fig. 3(c) for films with 5% of

fibers, the corresponding DDR, from left to right, are 16.2, 14.4 and 12.5 respectively. The film processed with the smallest DDR shows a large error in lay flat width. This means that this process condition delimits the processability window. Overall, if one exclude this latter film with 5% fibers, the data in Fig. 3 indicate that better bubble stability is achieved with the composites, as deviations in films thickness and half width are significantly larger for PLA films.
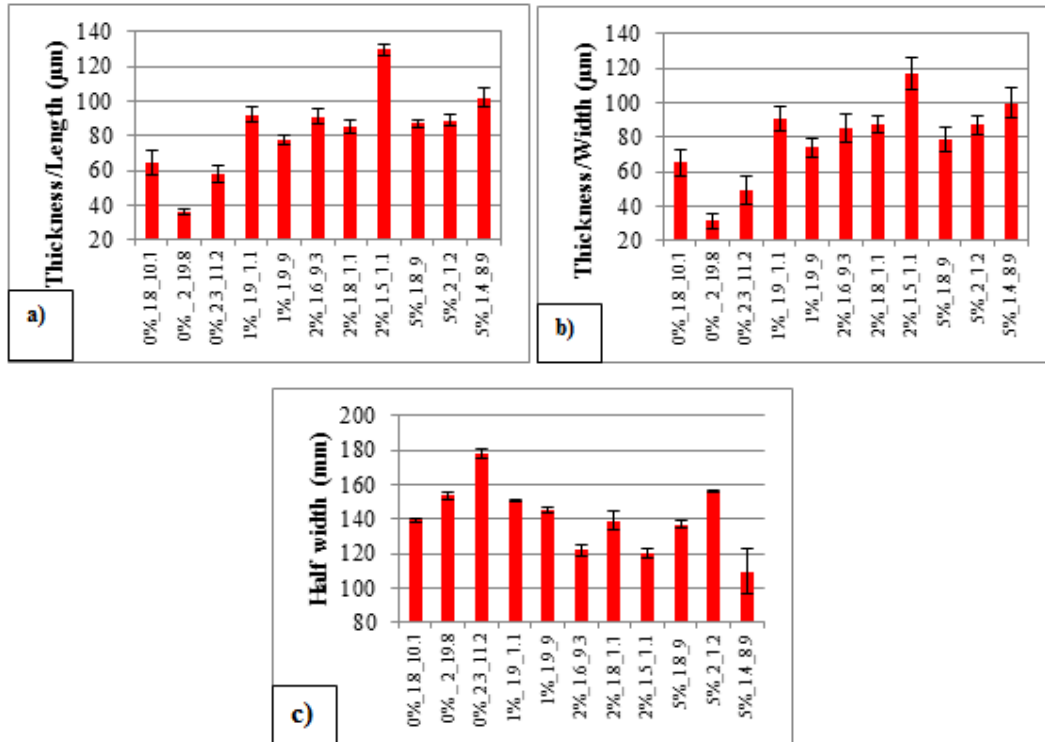

Figure 3: Average film thicknesses along the length (a) and along the width (b), and average half lay-flat width (c) measured for all blown films labeled as DPLF content in wt. %_BUR_TUR. The computation of means and errors is described in the text
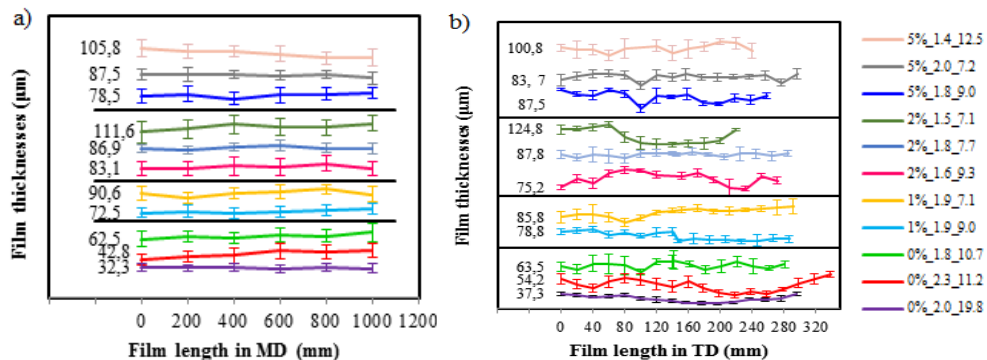

Figure 4: Spatial variation of average films thicknesses: (a) along the machine direction (MD, statistics on 12 points up to 18 points along the film width, depending on BUR), and (b) along the transverse direction (TD, statistics on 6 points along one meter film length)

3.2 Morphological Analysis

Optical microscopy imaging of selected sample films was performed in order to investigate fiber distribution in the films. The micrographs in Figs. 5(a)-5(b) refer to films containing 5% of fibers at two different magnifications. It demonstrates that fibers seem to be uniformly distributed in the film. The

comparison between images taken in light (Fig. 5(c)) and dark (Fig. 5(d)) bands of the films (as seen in Fig. 2) indicates that no differences in fiber content or distribution exist. Thus, the alternation of dark and light bands in the film does not result from changes in fiber concentration, but relates to variations in film thickness. A similar conclusion was achieved for films formulated with 1% DPLF.
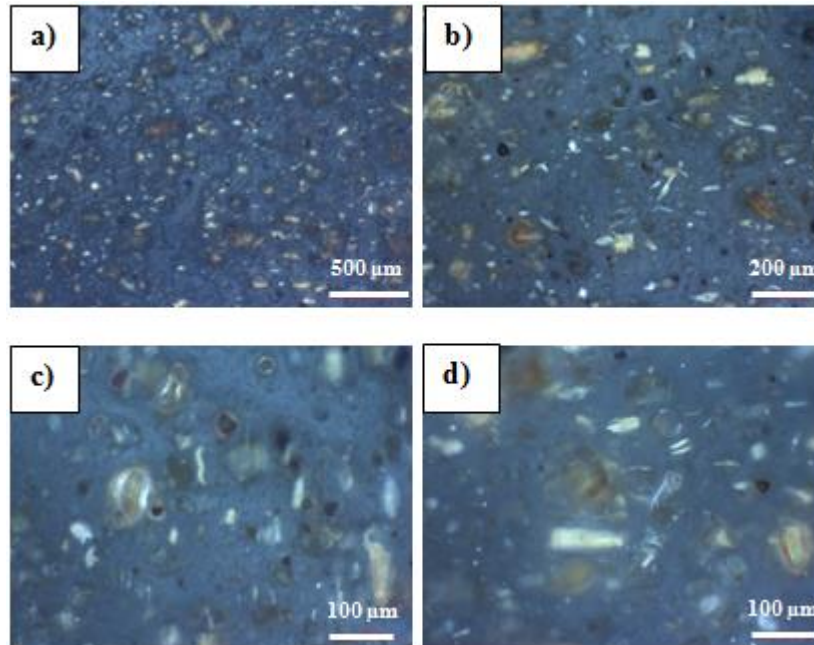

Figure 5: Optical microscopy images of (a) and (b) PLA/5% DPLF composite film at two different magnifications and of the same film cut in (c) a light band and in (d) a dark band

SEM investigations into the tensile fractured surfaces of the composite films are illustrated in Fig. 6. The images show the existence of micro voids. Fiber pull-outs and debonding holes are also observed, which relate to a poor adhesion between the fiber and the matrix. This was expected as no DPLF chemical treatment to improve the interfacial interactions with PLA has been performed. As the main objective here is the production of a low cost PLA based film, costly modification of DPLF was not considered. The orientation of plate-like fibers standing out the fractured section, and even the direction of the debonding holes, reveal that the fibers are lying in the plane of the film with no preferred orientation along MD or TD. The absence of fiber orientation is associated with the combined lack of stress transmission between fibers and PLA and the small BUR and TUR used during film blowing. Indeed BUR and TUR were not large enough to impart anisotropy to the films crystalline properties. This lack of crystalline anisotropy is reported in Tab. 1. The same degree of crystallinity was computed from WAXD spectra of films sampled along TD and MD. Data in Tab. 1 also indicate that the degree of crystallinity X decreases with the amount of DPLF compounded with PLA.
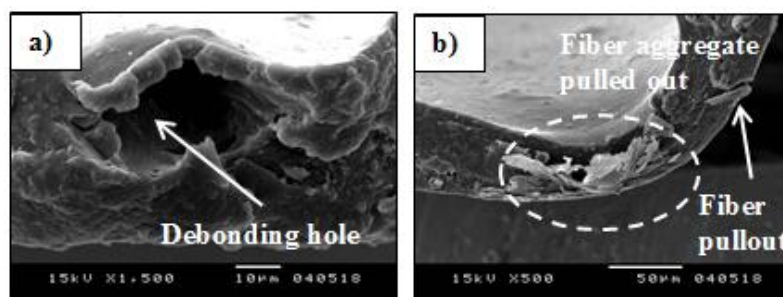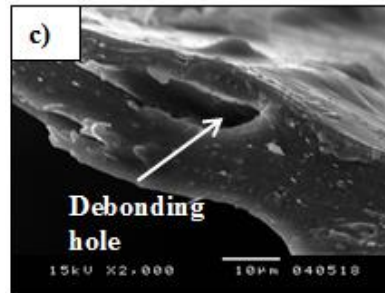
Figure 6: SEM images of the fractured surface (during tensile testing) of films with 1% (a) 2% (b) and 5% DPLF_1(c)

3.3 Mechanical Properties

An earlier report on biocomposite films produced with the same film blowing line under processing conditions nearly similar to those reported in Tab. 1, showed that BUR had no impact on the film mechanical properties, whereas films blown with larger TUR exhibited only larger Young's moduli [30]. Here, the small processability window of the composites impedes the production of films with significant differences in BUR and TUR (see Tab. 1). Thus, the impact of processing conditions on film mechanical properties could not be studied. Films produced with the most stable blowing process, and thus showing less spatial variation in both thickness and lay flat width, and having roughly similar thickness, were selected for mechanical characterization. Fig. 7 shows that the addition of DPLF to the PLA matrix affects the film mechanical properties. Incorporating 1% and 2% of fibers resulted in an increase of about 30% and 10%, respectively, in the films' Young moduli. For larger DPLF content, a reduction of about 42% is however found, which contrasts with the reinforcing effect observed for lower DPLF loads. We can also note a progressive decrease in both tensile strength and strain at break with the addition of DPLF (Figs. 7(b) and 7(c)) [31,32]. The lack of interfacial strength resulting from the bad adhesion between PLA and DPLF inhibits stress transfer and thus reduces the tensile strength [14,33,34]. The discontinuities and defects (voids) at the filler-matrix interface also restrict the mobility and the deformability of polymer chains, thereby causing lower elongation at break [14]. However, bad fiber-PLA interface should negatively impact the tensile strength, and to a lesser extent the Young's modulus, even at 1% fiber, which is in contrast to the reinforcing effect shown in Fig. 7 for such DPLF content. We therefore suspect that the reduction in mechanical properties at larger DPLF content is related with the fiber-induced loss in film crystallinity (see X in Tab. 1) and PLA thermal degradation during compounding with the DPLF fibers. To address the latter, the thermogravimetric analysis (TGA) of composites pellets was performed using a TA Q50 apparatus (TA Instruments) under a nitrogen flux. About 10-15 mg of sample were first heated at 50ºC during 10 minutes and the temperature was then swept from 50ºC to 600ºC at a heating rate of 20ºC/min. The temperature for maximum rate of degradation (Td) was determined from the time derivative of TGA thermograms with a precision of 0.5ºC. Td for the processed PLA material is 333.8ºC, whereas Td of DPLF composites are 332.4ºC, 331.0ºC and 316.8ºC for 1, 2 and 5% of fibers, respectively. The fact that Td shows up at smaller temperatures indicate that the addition of natural fibers reduces the overall thermal stability of the PLA matrix. Therefore, the reinforcing effect triggered by DPLF fiber at lower contents (1 and 2%) is balanced by the fiber-enhanced degradation of the PLA matrix, which is more pronounced at 5%. Altogether, at 5% fiber, both loss in PLA crystallinity and PLA degradation overcome the DPLF reinforcing effect, thereby explaining the drop in films mechanical properties after an initial improvement of such properties up to 2% fiber loading.
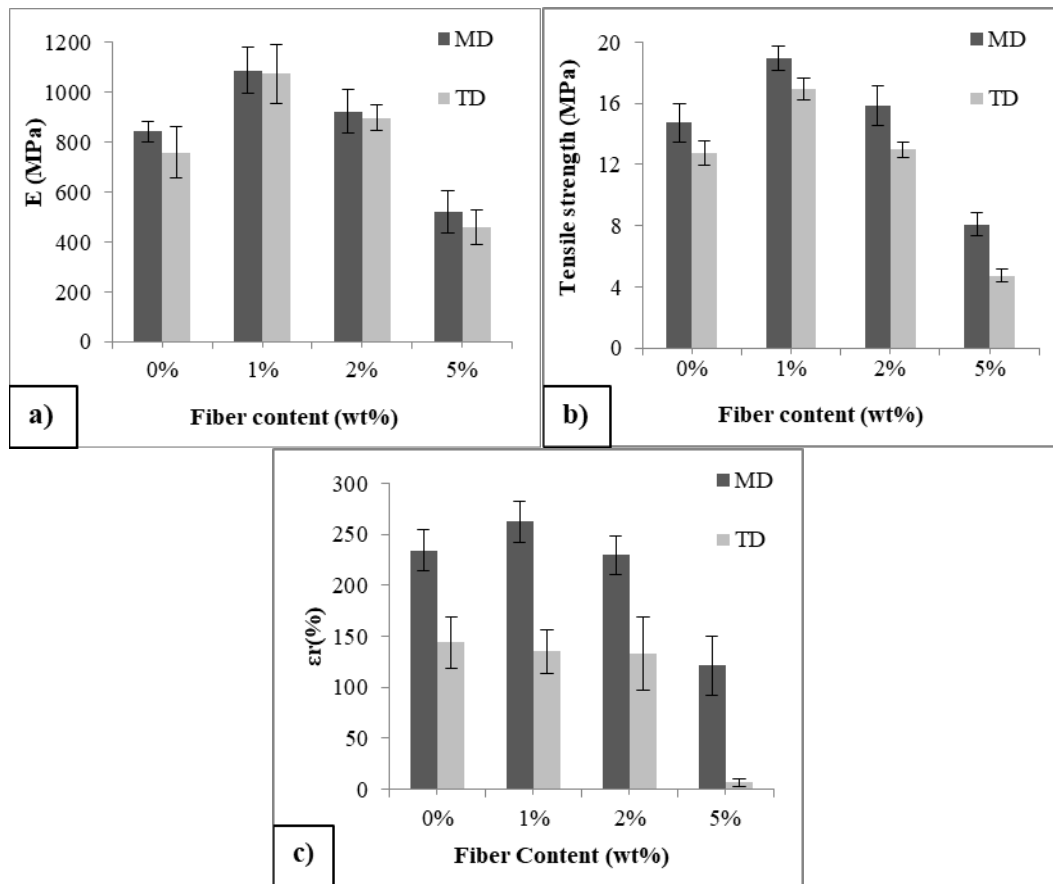
Figure 7: Film mechanical properties (Young modulus (a), Tensile strength (b) and elongation at break εr (c)) as a function of DPLF content

Fig. 7 shows as well some anisotropy in mechanical properties, which is more obvious in the deformation at break values. Two factors may explain this anisotropy: structural orientation in the film and/or the thickness instability, which is more developed along TD (see Figs. 3 and 4). To get an answer for this problematic, an anisotropy index computed as $Anisotropy\ index\ (\%) = \frac{mean\ strain\ at\ break\ in\ MD - mean\ strain\ at\ break\ in\ TD}{mean\ strain\ at\ break\ in\ MD}$, is reported in Tab. 2 for all films mechanically tested, together with the relative variation of film thickness along TD, which is computed as $Relative\ thickness\ variation\ (\%) = \left(\frac{Thickness\ standard\ deviation\ along\ TD}{mean\ thickness\ along\ TD}\right)$. We can thus observe from the data in Tab. 2 that the anisotropy index is the largest for the composite with 5% of fibers. Remarkably, for this film, the thickness variability is not the largest one. This trend thus suggests that the mechanical anisotropy in composite films is rather controlled by the fiber content. Wide angle X-ray diffraction spectra showed that the crystallinity of produced films is the same along TD and MD, see Tab. 1. The analysis of morphologies pictured in Figs. 5 and 6 indicate the absence of DPLF orientation along MD or TD. We are thus left with polymer chain orientation along MD in the film amorphous phase to explain the larger strain at break along MD. If one conjectures that fibers promote polymer chain orientation along MD due to local enhancement of deformation rates by chain confinement, then we can expect a progressive increase in the anisotropy index with further addition of fiber. However, for 1% and 2% composites, mechanical anisotropy seems to be roughly the same as the one exhibited by the neat PLA film, which in turn presents the largest relative thickness variation. This latter result indicates that mechanical anisotropy in neat PLA film is promoted (to catch up with composites at 1% and 2%) by the thickness variability. In conclusion, the 2 factors seem to affect simultaneously the mechanical anisotropy

of the films and in a differentiated way depending on whether the film is filled with fibers or not. Further investigations are needed to study the effect of each factor on the film mechanical anisotropy.

Table 2: Relative thickness variation along TD and anisotropy index of the strain at break of PLA and composite films

Fiber content (wt.%)	0	1	2	5
Relative thickness variation (%)	15.9	8	5.8	6.4
Anisotropy index (%)	39	48	42	94

Fig. 8 shows the load *vs.* displacement curves of a film with 5% DPLF cut in MD and a film with 2% DPLF cut in TD. Images of film samples pictured at various times during the tensile testing are also inserted in Fig. 8. Tensile curves show a linear elastic region, then, a yielding zone followed by a drop in stress, a formation of a neck, an increase in stress and finally fracture. The inserted photos in Fig. 8(a) show a nucleation and propagation in a scattered way of white patches, indicating a damaging of the material under loading. The relatively homogeneous, and therefore non-localized, appearance of this damage conforms with the relatively small thickness variation in the MD direction and also the homogeneous fiber distribution. The opposite would have favored a more localized damage. For the second film cut in TD (Fig. 8(b)), the strain may not be uniformly distributed, as damaged (whitish) and undamaged zones (dark) alternate. Hence, light bands (bands with reduced thickness) turn whitish earlier during the loading and will be a location of strain concentration wherein the film will break-up.
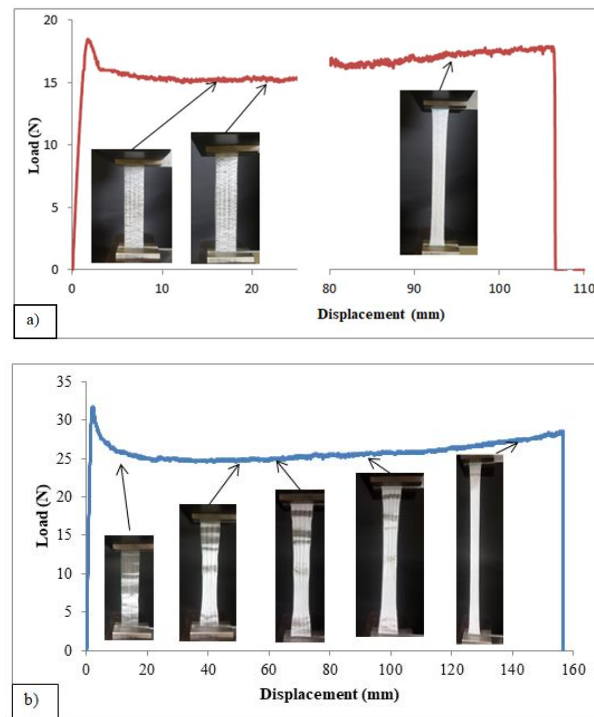

Figure 8: Load *vs.* Displacement curves for (a) film with 5% of fiber cut in MD and (b) film with 2% of fiber cut in TD with photos of the corresponding films captured at different stages of deformation

4 Conclusions

In this work, composite films based on PLA matrix containing DPLF as filler were produced by film blowing process. DPLF has a reinforcing effect on PLA film until 2% of filler with an optimum around 1%. Beyond this filler load, mechanical properties of the composite films decrease. This is due to intrinsic material factors such as the loss in the film crystallinity and the PLA thermal degradation both triggered by DPLF addition, as well as the increasing effect of the weak interface between the fiber and the matrix. Chemical modification or use of adhesion promoters can be interesting paths to improve the overall mechanical properties [35,36]. It was also noted that film tensile properties in TD were lower than in MD. This was explained by the fact that amorphous polymer chains were more oriented in the MD, and also by the gauge variation/thickness instability along TD, which was reduced upon addition of DPLF.

References

1. Farah, S., Anderson, D. G., Langer, R. (2016). Physical and mechanical properties of PLA, and their functions in widespread applications-A comprehensive review. *Advanced Drug Delivery Reviews, 107,* 367-392.

2. Bindhu, B., Renisha, R., Roberts, L., Varghese, T. O. (2018). Boron nitride reinforced polylactic acid composites film for packaging: preparation and properties. *Polymer Testing, 66,* 172-177.

3. Al-Itry, R., Lamnawar, K., Maazouz, A. (2012). Improvement of thermal stability, rheological and mechanical properties of PLA, PBAT and their blends by reactive extrusion with functionalized epoxy. *Polymer Degradation and Stability, 97(10),* 1898-1914.

4. Al-Itry, R., Lamnawar, K., Maazouz, A. (2014). Reactive extrusion of PLA, PBAT with a multi-functional epoxide: Physico-chemical and rheological properties. *European Polymer Journal, 58,* 90-102.

5. Debeli, D. K., Guo, J., Li, Z., Zhu, J., Li, N. (2017). Treatment of ramie fiber with different techniques: the influence of diammonium phosphate on interfacial adhesion properties of ramie fiber-reinforced polylactic acid composite. *Iranian Polymer Journal (English Edition), 26(5),* 341-354.

6. Scaffaro, R., Maio, A., Sutera, F., Gulino, E. F., Morreale, M. (2019). Degradation and recycling of films based on biodegradable polymers: a short review. *Polymers, 11(4),* 651.

7. Scaffaro, R., Maio, A., Lopresti, F. (2019). Effect of graphene and fabrication technique on the release kinetics of carvacrol from polylactic acid. *Composites Science and Technology, 169,* 60-69.

8. Scaffaro, R., Botta, L., Maio, A., Gallo, G. (2017). PLA graphene nanoplatelets nanocomposites: physical properties and release kinetics of an antimicrobial agent. *Composites Part B: Engineering, 109,* 138-146.

9. Scaffaro, R., Maio, A. (2019). Integrated ternary bionanocomposites with superior mechanical performance via the synergistic role of graphene and plasma treated carbon nanotubes. *Composites Part B: Engineering, 168,* 550-559.

10. Teixeira, P. F., Sutera, F., Scaffaro, R., Covas, J. A., Hilliou, L. (2019). Multi-parameter in-process monitoring of clay dispersion during melt compounding with PLA. *Express Polymer Letters, 13(3),* 276-285.

11. Scaffaro, R., Lopresti, F., Botta, L. (2018). PLA based biocomposites reinforced with Posidonia oceanica leaves. *Composites Part B: Engineering, 139,* 1-11.

12. Qin, L., Qiu, J., Liu, M., Ding, S., Shao, L. et al. (2011). Mechanical and thermal properties of poly(lactic acid) composites with rice straw fiber modified by poly(butyl acrylate). *Chemical Engineering Journal, 166(2),* 772-778.

13. Murariu, M., Dubois, P. (2016). PLA composites: from production to properties. *Advanced Drug Delivery Reviews.*

14. Khan, B. A., Na, H., Chevali, V., Warner, P., Zhu, J. et al. (2018). Glycidyl methacrylate-compatibilized poly(lactic acid)/hemp hurd biocomposites: processing, crystallization, and thermo-mechanical response. *Journal of Materials Science and Technology, 34(2),* 324-334.

15. Gil-Castell, O., Badia, J. D., Kittikorn, T., Strömberg, E., Ek, M. et al. (2016). Impact of hydrothermal ageing on the thermal stability, morphology and viscoelastic performance of PLA/sisal biocomposites. *Polymer Degradation and Stability, 132,* 87-96.

16. Sujaritjun, W., Uawongsuwan, P., Pivsa-Art, W., Hamada, H. (2013). Mechanical property of surface modified natural fiber reinforced PLA biocomposites. *Energy Procedia, 34,* 664-672.

17. Qian, S., Zhang, H., Yao, W., Sheng, K. (2018). Effects of bamboo cellulose nanowhisker content on the

morphology, crystallization, mechanical, and thermal properties of PLA matrix biocomposites. *Composites Part B: Engineering, 133,* 203-209.

18. Sung, S. H., Chang, Y., Han, J. (2017). Development of polylactic acid nanocomposite films reinforced with cellulose nanocrystals derived from coffee silverskin. *Carbohydrate Polymers, 169,* 495-503.

19. Herrera, N., Salaberria, A. M., Mathew, A. P., Oksman, K. (2015). Plasticized polylactic acid nanocomposite films with cellulose and chitin nanocrystals prepared using extrusion and compression molding with two cooling rates: effects on mechanical, thermal and optical properties. *Composites Part A, 83,* 89-97.

20. Herrera, N., Roch, H., Salaberria, A. M., Pino-orellana, M. A., Labidi, J. et al. (2016). Functionalized blown films of plasticized polylactic acid/chitin nanocomposite : Preparation and characterization. *Materials & Design, 92,* 846-852.

21. Karkhanis, S. S., Stark, N. M., Sabo, R. C., Matuana, L. M., Service, F. et al. (2018). Performance of poly (lactic acid)/cellulose nanocrystal composite blown films processed by two different compounding approaches. *Polymer Engineering & Science, 58(11),* 1965-1974.

22. Scaffaro, R., Botta, L., Lopresti, F., Maio, A., Sutera, F. (2017). Polysaccharide nanocrystals as fillers for PLA based nanocomposites. *Cellulose, 24(2),* 447-478.

23. Observatoire National de l'Agriculture. (n.d.). http://www.onagri.nat.tn/articles?id=5.

24. El may, Y., Jeguirim, M., Dorge, S., Trouvé, G., Said, R. (2012). Study on the thermal behavior of different date palm residues: characterization and devolatilization kinetics under inert and oxidative atmospheres. *Energy, 44(1),* 702-709.

25. Carneiro, O. S., Reis, R., Covas, J. A. (2008). Small-scale production of co-extruded biaxially oriented blown film. *Polymer Testing, 27(4),* 527-537.

26. Jung, H., Hyun, J. (2004). Fiber spinning and film blowing instabilities. *Polymer Processing Instabilities: Control and Understanding,* 321-387.

27. Jones, D. P. (2012). Methods of reducing roll faults caused by poor thickness profile. https://www.aimcal.org/uploads/4/6/6/9/46695933/jones_abs.pdf.

28. Vlachopoulos, J., Castillo, R., Polychronopoulos, N., Tanifuji, S. (2012). Blown film dies. *Design of Extrusion Forming Tools,* 141-168.

29. Mallet, B., Lamnawar, K., Maazouz, A. (2014). Improvement of blown film extrusion of poly(lactic acid): structure-processing-properties relationships. *Polymer Engineering and Science, 54(4),* 840-857.

30. Cunha, M., Berthet, M., Pereira, R., Covas, J. A., Vicente, A. A. et al. (2014). Development of polyhydroxyalkanoate/beer spent grain fibers composites for film blowing applications. *Polymer Composites, 36(10),* 1859-1865.

31. Morreale, M., Scaffaro, R., Maio, A., Mantia, F. P. La. (2008b). Mechanical behaviour of Mater-Bi (R)/wood flour composites : a statistical approach. *Composites Part A, 39,* 1537-1546.

32. Morreale, M., Scaffaro, R., Maio, A., Mantia, F. P. La. (2008a). Effect of adding wood flour to the physical properties of a biodegradable polymer. *Composites Part A, 39,* 503-513.

33. Arrakhiz, F. Z., El Achaby, M., Malha, M., Bensalah, M. O., Fassi-Fehri, O. et al. (2013). Mechanical and thermal properties of natural fibers reinforced polymer composites: Doum/low density polyethylene. *Materials and Design, 43,* 200-205.

34. Spiridon, I., Darie, R. N., Kangas, H. (2016). Influence of fiber modifications on PLA/fiber composites. Behavior to accelerated weathering. *Composites Part B: Engineering, 92,* 19-27.

35. La Mantia, F. P., Morreale, M. (2011). Green composites: a brief review. *Composites Part A: Applied Science and Manufacturing, 42(6),* 579-588.

36. Wu, C. S., Liao, H. T., Cai, Y. X. (2017). Characterisation, biodegradability and application of palm fibre-reinforced polyhydroxyalkanoate composites. *Polymer Degradation and Stability, 140,* 55-63.